FULL PAPER

Dalton
www.rsc.org/dalton

The length, strength and polarity of metal–carbon bonds: dialkylzinc compounds studied by density functional theory calculations, gas electron diffraction and photoelectron spectroscopy †

Arne Haaland,*[a] Jennifer C. Green,*[b] G. Sean McGrady,*‡[c] Anthony J. Downs,[b] Emanuel Gullo,[c] Mark J. Lyall,[b] Jessima Timberlake,[b] Andrey V. Tutukin,[a] Hans Vidar Volden[a] and Kari-Anne Østby[a]

[a] *Department of Chemistry, University of Oslo, Box 1033, Blindern, N-0315 Oslo, Norway. E-mail: arne.haaland@kjemi.uio.no*

[b] *Inorganic Chemistry Laboratory, University of Oxford, South Parks Road, Oxford, UK OX1 3QR. E-mail: jennifer.green@chemistry.oxford.ac.uk*

[c] *Department of Chemistry, King's College London, Strand, London, UK WC2R 2LS*

Received 16th June 2003, Accepted 2nd September 2003
First published as an Advance Article on the web 19th September 2003

The molecular structures and thermodynamic functions of seven dialkyl zinc compounds, R_2Zn, R = Me, Et, *i*-Pr, *t*-Bu, *n*-Pr, neopentyl and the silaneopentyl Me_3SiCH_2, of the parent hydrocarbons RH and of the radicals R have been determined by density functional theory calculations at the B3LYP/SDD level. The molecular structures of the *i*-Pr, *t*-Bu, *neo*-Pe and Me_3SiCH_2 derivatives have been determined by gas electron diffraction. Me_2Zn, Et_2Zn, *t*-Bu_2Zn and *neo*-Pe_2Zn have been studied by photoelectron spectroscopy and the ionisation energies calculated. Both experimental and calculated Zn-C bond distances were found to increase in the order

$$Me_2Zn \approx (Me_3SiCH_2)_2Zn < Et_2Zn \approx n\text{-}Pr_2Zn \approx neo\text{-}Pe_2Zn < i\text{-}Pr_2Zn < t\text{-}Bu_2Zn.$$

Calculated mean bond rupture enthalpies indicate that the strength of the Zn–C bonds decrease in the same order, *viz*.

$$Me_2Zn \approx (Me_3SiCH_2)_2Zn > Et_2Zn \approx n\text{-}Pr_2Zn \approx neo\text{-}Pe_2Zn > i\text{-}Pr_2Zn > t\text{-}Bu_2Zn.$$

Both bond lengths and bond strengths were found to be strongly correlated with the inductive Taft constant I, indicating that the bond strength increases and the bond length decreases with increasing electron withdrawing power of the alkyl group. Evidence from the literature indicates that bond strengths and bond lengths in homoleptic alkyl derivatives of the main group metals in Groups 12, 13 and 14 and of the transition elements in Group 4 vary in the same manner.

Introduction

Dimethyl- and diethyl-zinc were apparently the first main group organometallic compounds to be synthesised and characterised; the events and deliberations leading up to their preparation by Frankland more than 150 years ago have recently been reviewed by Seyferth.[1]

The pure rotational Raman spectra of dimethylzinc and the Cd and Hg analogues, recorded by Rao *et al*.,[2] show that the molecules are symmetric tops, and thus confirm that the CMC fragments are linear as expected. The moments of inertia of $(CH_3)_2Zn$ and the fully deuterated molecule yielded a Zn–C bond distance of 192.9 ± 0.4 pm.[2] The electronic structure of Me_2Zn was studied by photoelectron (PE) spectroscopy and *ab initio* calculations 25 years ago.[3] The two highest occupied molecular orbitals were found to be the symmetric and antisymmetric C–Zn–C three-centre orbitals. The 3d electrons are essentially nonbonding. Mulliken population analysis indicated that the Zn atom carries a net positive, the C atoms a net negative charge.

Twenty years ago some of us determined the molecular structures of dimethyl-, diethyl- and di-*n*-propyl-zinc by gas electron diffraction (GED).[4] The Zn–C bond distance in Me_2Zn, r_a = 193.0(2) pm, was in excellent agreement with the spectroscopic value, while the Zn–C bond distances in Et_2Zn and *n*-Pr_2Zn were slightly, but significantly longer at 195.0(2) and 195.2(3) pm, respectively. It is known that the strength of the Zn–C bond, as measured by the Zn–C mean bond rupture enthalpy, is significantly greater in Me_2Zn than in Et_2Zn.[5]

The dialkyl derivatives of zinc are particularly well suited for a systematic investigation of how the metal-to-carbon bond length, bond strength, and polarity in metal alkyl compounds depend on the nature of the alkyl group R. Four factors contribute to this suitability. (i) There is a wide variety of compounds which are relatively easy to prepare. (ii) The compounds are persistently monomeric and sufficiently stable and volatile to be investigated by GED and photoelectron (PE) spectroscopy at ambient temperatures. (iii) The linearity of the CZnC fragment, in conjunction with the relatively long Zn–C bond distances, minimizes steric interactions between the two alkyl groups, so that only electronic effects are likely to be registered. (iv) If the alkyl group consists of C and H only, the Zn–C bond distance is well removed from other bonded or nonbonded distances in the

† Electronic supplementary information (ESI) available: tables of calculated and experimental (GED) root-mean-square amplitudes of vibration and figures showing experimental and calculated modified molecular intensity curves for *i*-Pr_2Zn, *t*-Bu_2Zn, *neo*-Pe_2Zn and $(Me_3SiCH_2)_2Zn$. See http://www.rsc.org/suppdata/dt/b3/b306840b/

‡ Current adress: Department of Chemistry, University of New Brunswick, Fredericton, NB E3B 6E2, Canada. smcgrady@unb.ca

DOI: 10.1039/b306840b

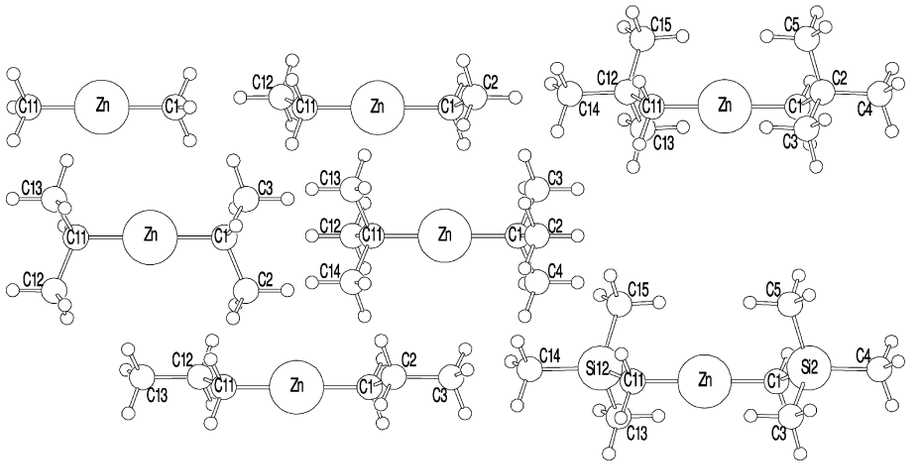

Fig. 1 The molecular structures of the dialkyl zinc compounds, R_2Zn, R = Me, Et, *i*-Pr, *t*-Bu, *n*-Pr (*anti,anti* conformer), *neo*-Pe and Me_3SiCH_2 as determined by DFT calculations at the B3LYP/SDD level. Each molecule has a twofold symmetry axis through the Zn atom and in the plane of the paper.

molecule, and so may be determined with good accuracy by GED. In this article, we report the results of (a) Density Functional Theory (DFT) calculations on seven zinc dialkyls, Me_2Zn, Et_2Zn, *n*-Pr_2Zn, diisopropylzinc, di-*tert*-butylzinc, dineopentylzinc and the β-silaneopentyl derivative $(Me_3SiCH_2)_2Zn$; (b) structure determinations of *i*-Pr_2Zn, *t*-Bu_2Zn, *neo*-Pe_2Zn and $(Me_3SiCH_2)_2Zn$ by GED, supplementing earlier studies; and (c) of photoelectron spectroscopic studies of Me_2Zn, Et_2Zn, *t*-Bu_2Zn, and *neo*-Pe_2Zn.

Results and discussion

Molecular structures of dialkylzincs

The molecular structures of R_2Zn, R = Me, Et, *i*-Pr, *t*-Bu, *n*-Pr, *neo*-Pe and Me_3SiCH_2 obtained by DFT structure optimisations at the B3LYP/SDD level are shown in Fig. 1. The most important bond distances and valence and dihedral angles are listed in Table 1, along with the corresponding parameters obtained by structure refinement to gas electron diffraction data in this work or from ref. 4 for R = Me, Et or *n*-Pr. When comparisons are made, it should be recalled that while optimisation by quantum chemical calculations yields equilibrium structure parameters, the bond distances and valence and dihedral angles obtained from the GED data have been averaged over the vibrations of the molecules in the molecular beam. Due to the anharmonicity of bond stretching vibrations, the vibrationally averaged (r_a) bond distances are normally some tenths of a pm longer than the equilibrium (r_e) bond distances, while vibrationally averaged valence angles and – in particular – dihedral angles larger than 90° may be significantly smaller than the equilibrium values. In the following we shall limit ourselves to a discussion of the molecular symmetries, the magnitude of the ∠CZnC valence angles, possible van der Waals interactions between alkyl groups, the barriers to internal rotation of the alkyl groups about the Zn–C bonds, and finally to the variation of Zn–C bond distances.

The equilibrium structures for Me_2Zn and *t*-Bu_2Zn obtained by DFT calculations both have D_{3d} symmetry. This implies that the CZnC angles are exactly 180° and that the H atoms in Me_2Zn and the Me groups in *t*-Bu_2Zn are staggered when viewed down the CZnC axis.

The molecular symmetries of Et_2Zn, *i*-Pr_2Zn, *neo*-Pe_2Zn or $(Me_3SiCH_2)_2Zn$ depend on the relative orientations of the two ligands, that is on the dihedral angles τ(C(2)C(1)C(11)C(12)) = $\tau(C_\beta C_\alpha C_\alpha' C_\beta')$ in Et_2Zn or *neo*-Pe_2Zn, and on the corresponding dihedral angles $\tau(HC_\alpha C_\alpha' H')$ or $\tau(SiC_\alpha C_\alpha' Si')$ in *i*-Pr_2Zn or $(Me_3SiCH_2)_2Zn$, respectively. If the dihedral angle is zero, the molecular symmetry is C_{2v}: if it is 180°, the molecular symmetry is C_{2h}.

DFT structure optimisation of the four last compounds yielded equilibrium structures of C_2 symmetry with dihedral angles $\tau(C_\beta C_\alpha C_\alpha' C_\beta')$, $\tau(HC_\alpha C_\alpha' H')$, or $\tau(SiC_\alpha C_\alpha' Si')$ ranging from 146 to 167°. Even though the molecular symmetries do not require the CZnC axes to be linear, all CZnC angles are calculated to be larger than 179.0°. Since steric interactions between the asymmetrically positioned alkyl ligands might change the CZnC valence angle, the near-linearity of the CZnC skeleton in these compounds may be interpreted as a first indication that such interactions are negligible. This conclusion is confirmed by examination of the distances between C atoms in different alkyl ligands. With the exception of $C_\alpha \cdots C_\alpha$ distances, these are all about 450 pm or longer as compared with a methyl group van der Waals diameter of 400 pm. It is clear therefore that the equilibrium structures are *not* destabilised by steric repulsion between alkyl groups, and that the variation of mean Zn–C bond rupture enthalpies (see below) cannot be due – wholly or in part – to steric repulsion between the ligands.

We now turn our attention to the barriers restricting internal rotation of the alkyl groups about the Zn–C bonds. The threefold barriers in Me_2Zn or *t*-Bu_2Zn obtained by optimisation of molecular models of D_{3h} symmetry, that is with eclipsed H atoms or Me groups, were of the order of 0.10 kJ mol^{-1}. The only distances to change during internal rotation in Me_2Zn are non-bonded H ⋯ H distances which leave very little trace in the GED data. The GED structure refinement of Me_2Zn was therefore carried out on a D_3 model in which the largest dihedral angle of type τ(HCCH) was fixed at 150°, *i.e.* intermediate between staggered (τ = 180°) and eclipsed (τ = 120°) models. For *t*-Bu_2Zn we carried out the structure refinement under D_3 symmetry with a variable torsional angle. The thermal average angle thus obtained, $\tau_a(C_\beta C_\alpha C_\alpha' C_\beta')$ = 124(8)°, might be taken as an indication that the equilibrium structure is eclipsed rather than staggered, but is hardly sufficient to prove that it is so.

The barrier to internal rotation of the alkyl groups in Et_2Zn was explored by carrying out a relaxed scan of the potential energy surface with the torsional angle $\tau(C_\beta C_\alpha C_\alpha' C_\beta')$ varied from 0 to 180° in steps of 10°. The highest energy, 0.25 kJ mol^{-1} above the equilibrium structure, was obtained for $\tau(C_\beta C_\alpha C_\alpha' C_\beta')$ = 0°, *i.e.* for the *syn* conformation. It should be noted, however, that because of the linearity of the CZnC skeleton, the distances between β-C atoms at opposite ends of the molecule in *t*-Bu_2Zn, *i*-Pr_2Zn or Et_2Zn are larger than 480 pm for any relative orientation of the alkyl groups. This is too large for steric repulsions to make any significant contribution to the rotational barriers.

Table 1 Molecular structures of dialkylzincs, R_2Zn, obtained by DFT calculations at the B3LYP/SDD level and gas electron diffraction (GED). Molecular point groups, bond distances, valence angles, dihedral angles τ, and highest barriers to internal rotation of the alkyl groups about the Zn–C bonds max; $V(\tau)$.

	Me_2Zn		Et_2Zn		*i*-Pr_2Zn		*t*-Bu_2Zn	
	DFT	GED[a]	DFT	GED[a]	DFT	GED	DFT	GED
Symmetry	D_{3d}	D_3	C_2	C_2	C_2	C_2	D_{3d}	D_3
Bond distances/pm	r_e	r_a	r_e	r_a	r_e	r_a	r_e	r_a
Zn–C	194.5	193.0(2)	196.0	195.0(2)	197.5	196.1(3)	198.8	197.4(3)
C_α–C_β	110.0[b]	110.0(5)[b]	155.5	154.0(3)	155.3	153.6(2)	155.2	154.3(2)
Valence angles/°	$\angle_e$	$\angle_a$	$\angle_e$	$\angle_a$	$\angle_e$	$\angle_a$	$\angle_e$	$\angle_a$
CZnC	180.0	180.0	179.9	180.0	179.9	178.0(7)	180.0	180.0
$ZnC_\alpha C_\beta$	110.8[c]	112.5(5)[c]	114.2	114.5(3)	111.8[e]	112.0(2)	109.8	110.3(2)
$C_\beta C_\alpha C_\beta'$	–	–	–	–	110.9	110.8(4)	109.2	108.7(2)
Dihedral angles/°	τ_e	τ_a	τ_e	τ_a	τ_e	τ_a	τ_e	τ_a
Barriers/kJ mol^{-1}	0.10	–	0.26	–	–	–	0.07	–
$C_\beta C_\alpha C_\alpha' C_\beta'$	180[d]	[150][d]	157	79(12)	146[d]	134(6)[d]	180	124(8)
	n-Pr_2Zn *aa*		*n*-Pr_2Zn g_+g_-		*neo*-Pe_2Zn		$(Me_3SiCH_2)_2Zn$	
	DFT	GED[a]	DFT	GED[a]	DFT	GED	DFT	GED
Symmetry	C_2	–	C_i	–	C_2	C_2	C_2	C_2
Bond distances/pm	r_e	r_a	r_e	r_a	r_e	r_a	r_e	r_a
Zn–C	196.0	195.2(3)	196.3	195.2(3)	196.3	196.0(3)	194.8	193.5(6)
C_α–C_β	155.4	153.5(5)	155.4	153.5(5)	156.0	154.7(2)	190.9[f]	188.1(3)[f]
C_β–C_γ	154.6	153.5(5)	154.5	153.5(5)	155.2[e]	153.9(2)[e]	191.4[g]	188.7(3)[g]
Valence angles/°	$\angle_e$	$\angle_a$	$\angle_e$	$\angle_a$	$\angle_e$	$\angle_a$	$\angle_e$	$\angle_a$
CZnC	180.0	180.0	[180]	180.0	179.4	180(2)	179.9	172(4)
ZnCC	114.5	114.5(5)	114.6	114.5(5)	115.6	116.0(3)	115.0[h]	112.8(2)[h]
$C_\alpha C_\beta C_\gamma$	113.0	114(2)	113.3	114(2)	110.0[e]	109.7(4)[e]	110.1[i,e]	112.2(4)[i,e]
$C_\gamma C_\beta C_\gamma'$	–	–	–	–	109.0[e]	109.3(4)[e]	108.8[j,e]	106.6(6)[j,e]
Dihedral angles/°	τ_e	τ_a	τ_e	τ_a	τ_e	τ_a	τ_e	τ_a
$C_\beta C_\alpha C_\alpha' C_\beta'$	157	–	180	–	147	93(3)	167[k]	81(6)[k]
$ZnC_\alpha C_\beta C_\gamma$	180	[180]	60	60(4)	180	175(4)	180[l]	172(4)[l]

[a] Ref. 4. [b] C–H. [c] ∠ZnCH. [d] $\tau(HC_\alpha C_\alpha' H')$. [e] Average value. [f] C_α–Si. [g] Si–C_γ. [h] ∠ZnCSi. [i] $\angle C_\alpha SiC_\gamma$. [j] $\angle C_\gamma SiC_\gamma'$. [k] $\tau(SiC_\alpha C_\alpha' Si')$. [l] $\tau(ZnC_\alpha SiC_\gamma)$.

No attempt was made to determine the barriers to internal rotation in *neo*-Pe_2Zn or $(Me_3SiCH_2)_2Zn$ through DFT calculations, but model calculations showed that rigid rotation of the alkyl groups will not lead to Me ··· Me distances smaller than 400 pm. It seems reasonable to assume, therefore, that the barriers restricting internal rotation of the alkyl groups about the Zn–C bonds are much smaller than the thermal energy at room temperature, RT = 2.5 kJ mol^{-1}, for all the compounds under consideration.

The GED structure refinements of Et_2Zn, *i*-Pr_2Zn, *neo*-Pe_2Zn and $(Me_3SiCH_2)_2Zn$ were all carried out under C_2 symmetry. The thermal average dihedral angles thus obtained ranged from $\tau_a(C_\beta C_\alpha C_\alpha' C_\beta') = 79(12)°$ in Et_2Zn to $\tau_a(HC_\alpha C_\alpha' H') = 134(6)°$ in *i*-Pr_2Zn. All are smaller than the calculated equilibrium values.

The GED data for *n*-Pr_2Zn showed that the molecular beam consisted of a mixture of molecules with *n*-PrZn fragments in *gauche* or *anti* conformations.[4] As part of this project, we optimised by DFT methods a model with both chains in *anti* conformations under C_2, and another model with one chain in a *gauche*$_+$ and the other in a *gauche*$_-$ conformation under C_i symmetry. The *anti*,*anti* conformer was found to be marginally more stable than the g_+g_- (by 2.1 kJ mol^{-1}). No minimum on the potential energy surface corresponding to a g_+g_+ conformer could be found. Since the primary aim of the calculations was to determine the Zn–C bond distances and bond enthalpies, we did not feel it necessary to optimise models with one *anti* and one *gauche* fragment.

Zn–C bond distances

In Fig. 2 we compare experimental radial distribution (RD) curves calculated from the gas electron diffraction data with the corresponding curves calculated for the best models obtained by the structure refinements. It is seen that while the peaks at about 195 pm representing the Zn–C bond distances are well resolved for the pure hydrocarbon alkyl compounds and the Zn–C bond distances consequently can be determined with good accuracy, the Zn–C and Si–C bond distance peaks in the

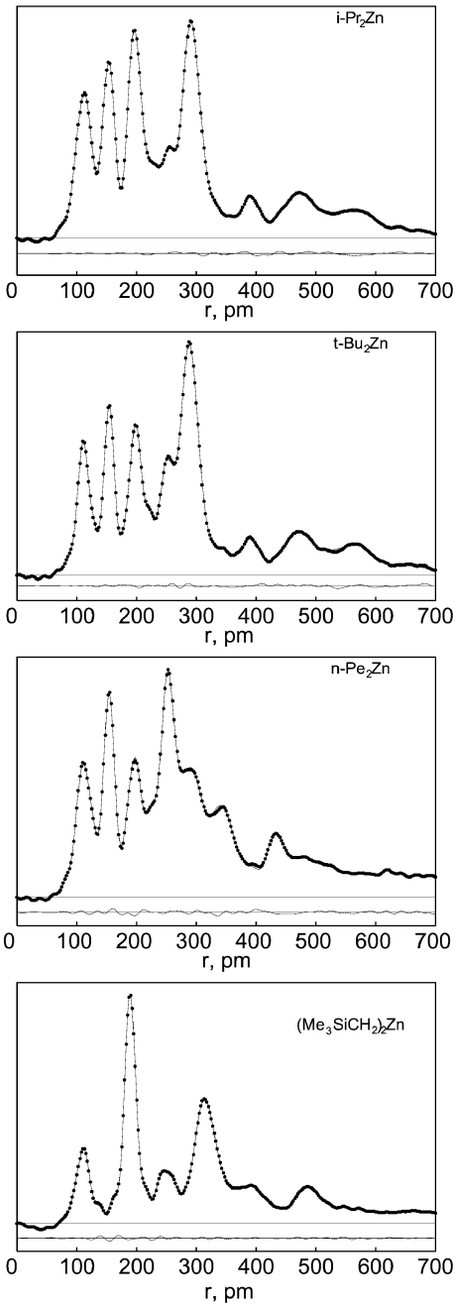

Fig. 2 Experimental (dots) and calculated (lines) radial distribution curves for (from top to bottom) *i*-Pr_2Zn, *t*-Bu_2Zn, *neo*-Pe_2Zn and $(Me_3SiCH_2)_2Zn$. Artificial damping constants $k = 25$ pm².

RD curve of $(Me_3SiCH_2)_2Zn$ are unresolved, and as a consequence the estimated standard deviation of the Zn–C bond distance is two or three times larger. As already mentioned, the true equilibrium bond distances are expected to be a few tenths of a pm shorter than the thermal average distances (r_a) obtained by GED. The equilibrium Zn–C bond distances obtained by DFT calculations on the seven dialkylzincs are, however, all a little longer than the r_a distances, the average difference being 1.1 pm. The main reason for this difference is undoubtedly a slight systematic overestimation of the calculated r_e distances. In Fig. 3 we plot the calculated r_e bond distances reduced by 1.1 pm, along with the experimental r_a bond distances with error bars equal to 2.5 estimated standard deviations. None of the experimental bond distances is significantly different from the calculated distances with offset. In the following we shall denote the calculated bond distances with offset as r without subscript. Three further features are apparent:

(i) The calculated Zn–C bond distances increase linearly with increasing number of Me groups attached to the α-C atoms,

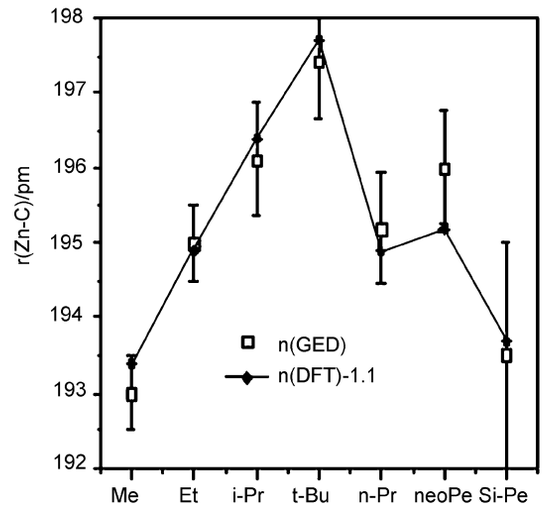

Fig. 3 Filled diamonds: calculated equilibrium Zn–C bond distances in R_2Zn, R = Me, Et, *i*-Pr, *t*-Bu, *n*-Pr, *neo*-Pe and Me_3SiCH_2 (Si–Pe) offset by subtraction of 1.1 pm. Squares: experimental (GED) bond distances with error bars corresponding to 2.5 estimated standard deviations.

from $r = 193.4$ pm in Me_2Zn to $r = 197.7$ pm in *t*-Bu_2Zn. This trend is confirmed by the experimental distances. The total elongation induced by three methyl groups is calculated to be 4.3 pm, the difference between the experimentally determined Zn–C bond distances in Me_2Zn and *t*-Bu_2Zn is 4.4(4) pm.

(ii) Me groups attached to the β-C appear to have much smaller effect on Zn–C bond distances than those attached to the α-C. The calculated Zn–C bond distance in the most stable conformer of *n*-Pr_2Zn differ from that calculated in Et_2Zn with less than 0.1 pm, the calculated bond distance in the less stable conformer is 0.3 pm longer. The difference between the experimental bond distances in the two compounds is 0.2(4) pm; The elongation induced by one methyl group on the β-C atom is clearly too small to be determined experimentally. The Zn–C bond distance in *neo*-Pe_2Zn where three methyl groups have been attached to the β-C, is calculated to be 0.5 pm longer than in Et_2Zn. The difference between the experimental bond distances in the two compounds is 1.0(4) pm. The elongation induced by three Me groups on the β-C is barely large enough to be detected experimentally and is much smaller than the elongation induced by three Me groups on the α-C;

(iii) Replacement of the β-C atom in *neo*-Pe_2Zn with a Si atom reduces the calculated bond distance by 1.7 pm. This shortening is confirmed by the GED results.

Thermochemistry and mean R–H and Zn–R bond rupture enthalpies

The mean Zn–R bond rupture enthalpy of a gaseous dialkyl zinc compound, D(Zn–R), may be calculated from the standard enthalpies of formation of the gaseous R_2Zn, the radical R and the Zn atom:

$$D(\text{Zn–R}) = 1/2\,[\Delta H^\circ_f(\text{Zn}) + 2\Delta H^\circ_f(\text{R}) - \Delta H^\circ_f(\text{R}_2\text{Zn})]$$

Standard enthalpies of formation of gaseous R_2Zn compounds, the radicals R and the parent hydrocarbons RH taken from the literature[6–8] are listed in Table 2. The ΔH°_f values for the hydrocarbons are known to within ±1 kJ mol^{-1}, but that of Me_3SiCH_3 carries an uncertainty of ±10 kJ mol^{-1}. The ΔH°_f values for the Me, Et, *i*-Pr, *n*-Pr and *t*-Bu radicals are all known to within ± 3 kJ mol^{-1}. Those of the *neo*-Pe and silaneopentyl (Me_3SiCH_2) radicals have been estimated,[8] but the estimates were based on assumed C–H bond rupture enthalpies for the parent hydrocarbons. In the worst case, we believe that the ΔH°_f value for the neopentyl radical may be off by as much as 10 kJ

Table 2 Dialkyl zinc compounds, R_2Zn. Standard enthalpies of formation, ΔH°_f of the hydrocarbons RH, the radicals R$^\bullet$ and R_2Zn all in the gas phase at 298 K.[a,b,c] Absolute standard enthalpies, H°_{298}, of R_2Zn, the hydrocarbon RH and the radical R$^\bullet$ at 298.15 K obtained by DFT calculations. Estimated standard enthalpies of formation of R$^\bullet$ based on reaction (1) and of R_2Zn based on reaction (4). R–H bond rupture enthalpies, D(R–H), and mean Zn–R bond rupture enthalpies based on literature data (in square brackets) and estimated bond rupture enthalpies based on reactions (1) and (4). Net atomic charges Q from Mulliken population analysis

	Me_2Zn	Et_2Zn	i-Pr_2Zn	t-Bu_2Zn
ΔH°_f[RH]/kJ mol^{-1}	[−74.5 ± 0.5][a]	[−83.8 ± 0.3][a]	[−104.7 ± 0.5][a]	[−134.2 ± 0.6][a]
ΔH°_f[R$^\bullet$]/kJ mol^{-1}	[147 ± 1][a]	[119 ± 2][a] 119 ± 8	[90 ± 2][a] 83 ± 8	[48 ± 3][a] 43 ± 8
ΔH°_f[R_2Zn]/kJ mol^{-1}	[53 ± 1][a]	[56 ± 4][a] 57 ± 8	32 ± 8	−17 ± 8
H°_{298}[RH]/MJ mol^{-1}	−106.2420	−209.3554	−312.4766	−415.6021
H°_{298}[R$^\bullet$]/MJ mol^{-1}	−104.5040	−207.6363	−310.7726	−413.9086
H°_{298}[R_2Zn]/MJ mol^{-1}	−805.7260	−1011.9306	−1218.1560	−1424.3962
D(R–H)/kJ mol^{-1}	[440 ± 1]	[421 ± 2] 421 ± 8	[413 ± 2] 406 ± 8	[400 ± 3] 395 ± 8
D(Zn–R)/kJ mol^{-1}	[186 ± 2]	[157 ± 4] 156 ± 8	132 ± 8	116 ± 8
Q(α–C)[R$^\bullet$]/au	−0.63	−0.41	−0.12	+0.30
Q(Zn)[R_2Zn]/au	+0.65	+0.52	+0.42	+0.39
Q(α–C)[R_2Zn]/au	−0.99	−0.62	−0.07	+0.09
	n-Pr_2Zn (aa)	n-Pr_2Zn (g_+g_-)	neo-Pe_2Zn	$(Me_3SiCH_2)_2Zn$
ΔH°_f[RH]/kJ mol^{-1}	[−104.7 ± 0.5][a]	[−104.7 ± 0.5][a]	[−167.4 ± 0.6][b]	[−246 ± 10][b]
ΔH°_f[R$^\bullet$]/kJ mol^{-1}	[100 ± 2][a] 99 ± 8	[100 ± 2][a] 99 ± 8	[31 ± ?][c,d] 39 ± 8	[−48 ± ?][c,d] −39 ± 8
ΔH°_f[R_2Zn]/kJ mol^{-1}	[17 ± 23][a] 10 ± 8	[17 ± 23][a] 11 ± 8	[−123 ± 17][c] −117 ± 8	[−355 ± 21][c] −306 ± 8
H°_{298}[RH]/MJ mol^{-1}	−312.4766	−312.4766	−518.7282	−1178.8494
H°_{298}[R$^\bullet$]/MJ mol^{-1}	−310.7569	−310.7569	−517.0055	−1177.1264
H°_{298}[R_2Zn]/MJ mol^{-1}	−1218.1777	−1218.1769	−1630.6820	−2950.9568
D(R–H)/kJ mol^{-1}	[423 ± 2] 421 ± 8	[423 ± 2] 421 ± 8	[416 ± ?][c,e] 424 ± 8	[416 ± ?][c,e] 425 ± 8
D(Zn–R)/kJ mol^{-1}	[157 ± 12] 159 ± 8	158 ± 8	[157 ± 17][c] 162 ± 8	[195 ± 21][c] 179 ± 8
Q(α–C)[R$^\bullet$]/au	−0.44	−0.44	−0.54	−0.83
Q(Zn)[R_2Zn]/au	+0.52	+0.43	+0.41	+0.60
Q(α–C)[R_2Zn]/au	−0.65	−0.62	−0.70	−1.13

[a] Ref. 6. [b] Ref. 7. [c] Ref. 8. [d] Based on an assumed value for D(R–H). [e] Assumed value.

mol^{-1}, and that of the silaneopentyl radical by as much as 20 kJ mol^{-1}. Accurate information on the dialkylzincs is even more sparse: the ΔH°_f of Me_2Zn has been determined with an uncertainty of ±1, that of Et_2Zn with an uncertainty of ± 4, those of n-Pr_2Zn, neo-Pe_2Zn and $(Me_3SiCH_2)_2Zn$ with estimated uncertainties of 23, 17 and 21 kJ mol^{-1}, respectively. The remaining ΔH°_f values appear to be unknown. Thermochemical data from the literature therefore permit the calculation of accurate mean Zn–R bond rupture enthalpies for Me_2Zn and Et_2Zn only.

A consistent set of R–H bond rupture enthalpies may be obtained from that of methane by using the absolute enthalpies obtained by the DFT calculations on the reactant and product molecules (see Table 2) to calculate the standard enthalpies of the isodesmic reactions

$$RH + CH_3 = R + CH_4 \quad (1)$$

This is equal to the difference between the R–H and Me–H bond rupture enthalpies:

$$\Delta H^\circ_r(1) = D(\text{R–H}) - D(\text{Me–H}) \quad (2)$$

Combination of the calculated enthalpy of the reaction with the literature value for the Me–H bond rupture enthalpy thus allows the calculation of D(R–H). The resulting values are listed in Table 2.

The reaction enthalpy $\Delta H^\circ_r(1)$ is also related to the enthalpies of formation through

$$\Delta H^\circ_r(1) = \Delta H^\circ_f(R) + \Delta H^\circ_f(CH_4) - \Delta H^\circ_f(RH) - \Delta H^\circ_f(CH_3) \quad (3)$$

The enthalpy of formation of the radical, $\Delta H^\circ_f(R)$, may thus be estimated from the calculated reaction enthalpy $\Delta H^\circ_r(1)$ in combination with literature values of the enthalpies of formation of the parent hydrocarbon, methane and the methyl radical. The resulting values are also listed in Table 2.

Similarly, a consistent set of mean Zn–C bond rupture enthalpies of the higher dialkylzincs may be obtained from that of Me_2Zn by using the DFT-based absolute enthalpies of reactants and products to calculate the standard enthalpy of the reaction

$$R_2Zn(g) + 2\,Me(g) = Me_2Zn(g) + 2\,R(g) \quad (4)$$

Combination of the calculated reaction enthalpies, $\Delta H^\circ_r(4)$, with the literature value of the mean Zn–C bond enthalpy in Me_2Zn allows the calculation of D(Zn–R) from

$$\Delta H^\circ_r(4) = 2\,D(\text{Zn–R}) - 2\,D(\text{Zn–Me}) \quad (5)$$

Finally, the reaction enthalpy $\Delta H^\circ_r(4)$ is related to the enthalpies of formation through

$$\Delta H^\circ_r(4) = \Delta H^\circ_f(Me_2Zn) + 2\Delta H^\circ_f(R) - \Delta H^\circ_f(ZnR_2) - 2\Delta H^\circ_f(Me) \quad (6)$$

and combination of the calculated reaction enthalpy with literature values for the enthalpies of formation of Me_2Zn and the Me and R radicals thus allows the estimation of the enthalpy of formation of the higher dialkylzincs. The resulting values are again listed in Table 2.

The R–H and Zn–R bond rupture enthalpies estimated in this manner depend on the calculated reaction enthalpies

$\Delta H^\circ_r(1)$ and $\Delta H^\circ_r(4)$, as well as on the literature values for the standard enthalpies of formation of Me_2Zn, methane, the methyl radical, and the H and Zn atoms, all of which have been determined with an accuracy of 1 kJ mol^{-1} or better. The errors associated with the DFT-based reaction enthalpies are difficult to assess, but since reactions (1) and (4) are isodesmic, systematic errors in individual absolute enthalpies may to some extent cancel. Comparison with the accurately literature values for the the R–H bond rupture enthalpies for R = Et, *i*-Pr, *t*-Bu and *neo*-Pe and the accurate literature value for *D*(Zn–Et) indicates that the DFT-based bond rupture enthalpies are accurate to within ±8 kJ mol^{-1}.

Fig. 4 is a scatterplot of the Zn–R bond enthalpies *vs.* the calculated Zn–C bond distances (with the −1.1 pm offset). It is seen that the regular increase of the bond distance with the number of methyl groups attached to the α-C atom is accompanied by an equally regular decrease of the bond strength. It should be noted, however, that while the Zn–C bond distance increases by less than 3% between Me_2Zn and *t*-Bu_2Zn, the mean bond enthalpy decreases by more than 35%! (Structure optimisation of Me_2Zn with the Zn–C distance fixed at the calculated value for *t*-Bu_2Zn, indicates that the energy increases with 12 kJ mol^{-1} which corresponds to a reduction of the mean bond enthalpy by less than 4%). On the other hand, introduction of Me groups on the β-C atom has little effect on the bond strength; the bond enthalpies of Et_2Zn, *n*-Pr_2Zn and *neo*-Pe_2Zn are indistinguishable. Finally, we note that not only is the Zn–C bond in $(Me_3SiCH_2)_2Zn$ nearly as short as that in Me_2Zn, it is also nearly as strong. Overall, there is a clear relationship between the bond distances and bond enthalpies; regression analysis yields a linear correlation coefficient of $\rho = -0.99$.

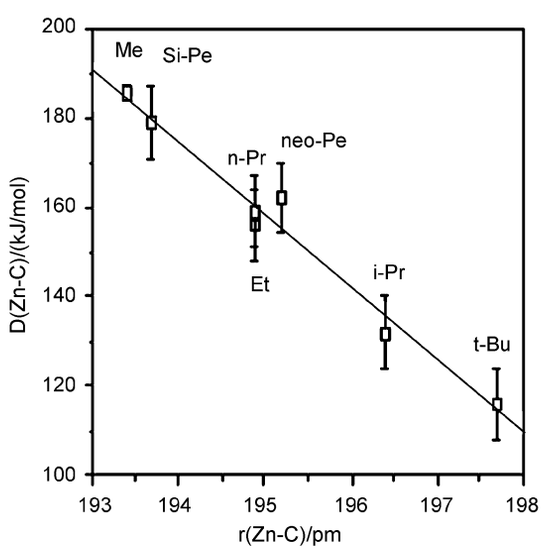

Fig. 4 Mean Zn–R bond rupture enthalpies as a function of Zn–C bond distances in dialkylzincs. Linear correlation coefficient $\rho = -0.99$.

Pilcher[9] and Smith[10] have suggested that the Zn–C bond rupture enthalpy of Et_2Zn is smaller than that of Me_2Zn because the relaxation energy of the Et radical is larger than the relaxation energy of the Me radical. The further weakening of the Zn–C bond when the number of Me groups attached to the α-C atom is increased to two or three might, of course, be explained in a similar manner. We have therefore estimated the relaxation energies by comparing the energies of the optimised radicals Me, Et, *i*-Pr and *t*-Bu with those obtained by single-point calculations on the radical structures adopted in the corresponding dialkylzinc compounds. The relaxation energies thus obtained fell in a remarkably narrow range from 39 to 42 kJ mol^{-1}. We conclude therefore that the calculated bond rupture enthalpies reflect the inherent strengths of the Zn–C bonds rather than the relaxation energies of the radicals.

Fig. 5 is a scatterplot of the R–H as a function of the Zn–R bond rupture enthalpies. The R–H and Zn–R bond strengths are clearly related, the linear correlation coefficient ρ being 0.97. It should be noted, however, that the variation of the Zn–R bond enthalpies is considerably larger than the variation of R–H bond enthalpies; 1.5 times larger in absolute terms and 3.6 times larger in relative terms. The correlation suggests that the variations of Zn–R and R–H dissociation enthalpies are caused by the same attribute of the alkyl groups, and we suggest that this attribute is the electronegativity or electron-withdrawing power. Bond distances are expected to decrease and bond rupture enthalpies to increase with increasing bond polarity, *i.e.* with increasing electron-withdrawing power of the alkyl group.[11]

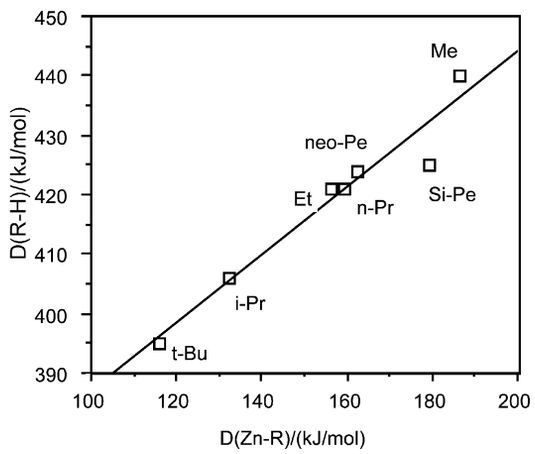

Fig. 5 C–H bond rupture enthalpies in alkanes RH as a function of mean Zn–C bond rupture enthalpy in dialkylzincs, R_2Zn. Correlation coefficient $\rho = 0.97$. If the point for Si–Pe = Me_3SiCH_2 is removed, the correlation coefficient increases to $\rho = 0.997$.

Taft and coworkers have used the free energies of proton-transfer reactions in the gas phase to derive a set of constants intended to gauge the relative electron-releasing powers and polarisabilities of various alkyl groups.[12] The first parameter *I* (for inductive) was intended to increase with increasing ability of the alkyl group to stabilise a molecule or molecular ion through electron release. Since the electron-releasing and withdrawing powers of an alkyl group are assumed to be inverse quantities, a high value of *I* corresponds to a low electron-withdrawing power. The second parameter *P* (for polarisability) was intended to increase with increasing ability of the alkyl groups to stabilise molecules through electrostatic interactions between the net charge on the nearest atom (or atoms) and the dipole moment that it induces on R. Polarisation effects are expected to be particularly important in molecules carrying net positive or negative charge. Fig. 6 is a scatterplot of the Zn–R bond

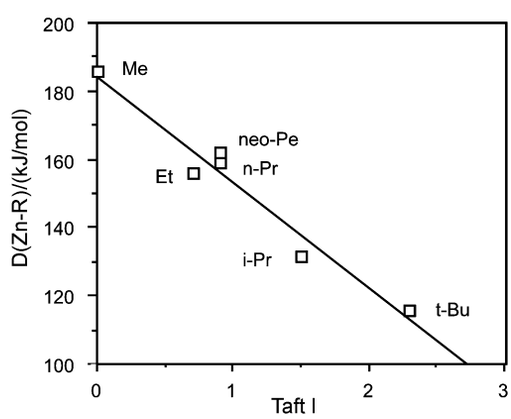

Fig. 6 Mean Zn–C bond rupture enthalpies in R_2Zn compounds as a function of the Taft inductive constant *I* of the alkyl group. $\rho = -0.98$.

Table 3 Orbital energies, calculated and experimental ionisation energies (eV) for R_2Zn, R = Me, Et, *t*-Bu and *neo*-Pe. For the 3d electrons the orbital energy and calculated IE are those of the δ symmetry orbital while the experimental IE is that of the band maximum

R_2Zn	Orbital energy		IE calc	IE exp
Me_2Zn	σ_u	−5.937	9.25	9.40
	σ_g	−7.775	11.16	11.36
	Zn d	−10.92	18.11	16.95
Et_2Zn	σ_u	−5.414	8.29	8.63
	σ_g	−7.075	9.89	10.46
	Zn d	−10.87	17.46	16.70
t-Bu_2Zn	σ_u	−4.752	7.34	7.80
	σ_g	−6.531	9.09	9.63
	Zn d	−10.76	17.38	16.13
neo-Pe_2Zn	σ_u	−5.323	8.00	8.33
	σ_g	−6.805	9.41	10.20
	Zn d	−10.72	17.43	16.30

enthalpies against the inductive Taft constants. A linear fit yields a correlation coefficient of −0.98. It is clear that the strength of the Zn–R bond increases with increasing electron-withdrawing power of the alkyl group.

On the other hand, the bond strength does not appear to depend on the polarisability of the alkyl groups: regression analysis yields a correlation coefficient of −0.75 between the Zn–R bond strengths and the Taft polarisability constants *P*. The magnitude of the correlation is in fact *smaller* than the correlation between the *I* and *P* parameters themselves for the alkyl groups under consideration ($\rho = 0.82$).

Mulliken population analyses of the wavefunctions of the dialkyl zinc compounds yield the net atomic charges for Zn and α-C atoms listed in Table 2. All the Zn atoms appear to carry positive charge, the magnitude of the charge increasing with increasing withdrawing power of the alkyl group. In order to understand the charges on the α-C atoms we begin with a discussion of the charge distribution in the free radicals R; Somewhat unexpectedly the more electron withdrawing radicals appear to be characterised by higher negative charge on the C atoms carrying the unpaired electron, see Table 2. The highest net negative charge on the α-C is found in the Me_3SiCH_2 (−0.83) followed by the Me radical (−0.63). The magnitude of the negative charge then decreases with decreasing electron withdrawing power of R, in *t*-Bu the α-C has acquired a net positive charge of +0.30. Comparison of the net charges on the α-C atoms in the R_2Zn compounds with those in the free radicals indicates that more than half the electron density released by the metal atom is retained by the α-C atoms which thus acquire an even larger negative charge. (The α-C atom in *t*-Bu_2Zn is left essentially neutral).

The polarity of the Zn–C bonds is perhaps best gauged by the magnitude of the negative product $-Q(Zn)Q(\alpha\text{-C})$. Indeed, linear fit of the mean bond rupture enthalpies $D(Zn–R)$ *vs.* this product yields a correlation coefficient of $\rho = 0.97$. The correlation coefficient for a linear fit of $-Q(Zn)Q(\alpha\text{-C})$ *vs.* the inductive and polarisability constants *I* and *P* are $\rho = -0.96$ and −0.83, respectively. It appears that the electronic ground state properties of bond length, bond strength and bond polarity are all determined primarily by the electron withdrawing power of the alkyl groups.

Photoelectron spectroscopy

The He I PE spectra of R_2Zn, R = Me, Et, *t*-Bu or *neo*-Pe, are shown in Fig. 7. Vertical ionisation energies are given in Table 3. For R = Me, Et and *t*-Bu, two low energy bands are evident and can be assigned to ionisation from the σ_u and σ_g Zn–C bonding orbitals. For *neo*-Pe_2Zn the second band forms a shoulder on the subsequent band but can just be distinguished. C–H and C–C ionisation bands lie below 16 eV with features that are characteristic of the respective alkyl groups. Zn 3d ionisations occur between 16 and 18 eV.

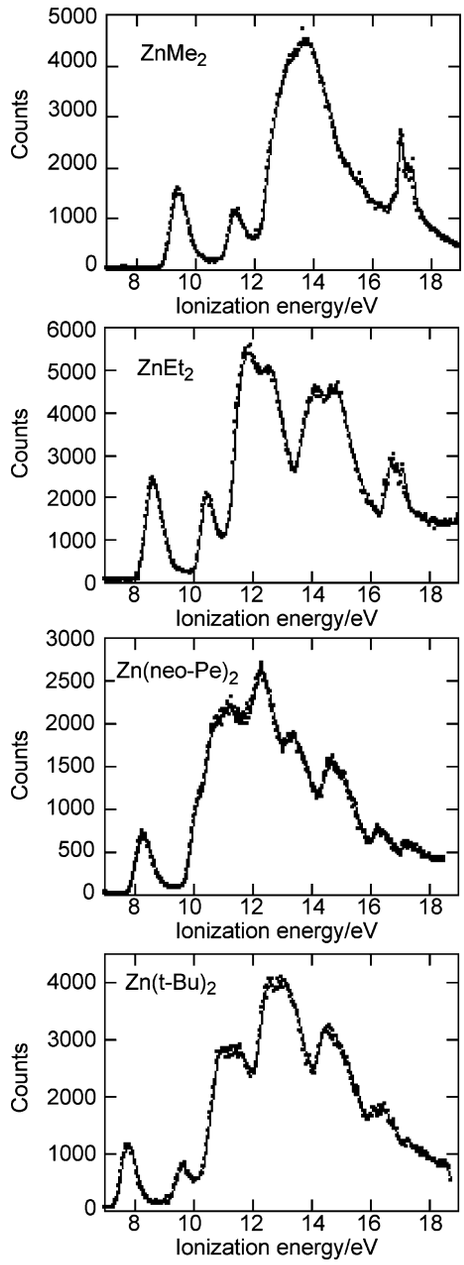

Fig. 7 He I photoelectron spectra of ZnR_2, R = Me, Et, *neo*-Pe and *t*-Bu.

The PE spectrum of Me_2Zn is in good agreement with that reported by Bancroft *et al.*[3] For the other dialkyls the 3d IE bands are less well resolved than for Me_2Zn and so they are each identified by the maximum in the 3d band, which corresponds to the $^2\Pi_{3/2}$ ion state in the earlier assignment. Calculated IEs are given for the σ_u and σ_g bands. Agreement for the σ_u band is within 0.3 eV and for the σ_g band within 0.6 eV. Calculation of the 3d ionisations proved complex. For the Me_2Zn cation, for example, the 3d character of the holes associated with the $^2\Sigma_g$ and $^2\Pi_g$ states were 63% and 75%, respectively. The $^2\Delta_g$ hole was 99% 3d, a physically more realistic estimate. The nodal properties of the 3d δ orbitals prevented mixing with methyl orbitals of the same formal symmetry (E_{1g} in the D_{3d} point group). The consequent ordering and spread of state energies for Me_2Zn was $^2\Delta < {}^2\Pi < {}^2\Sigma$. The experimental assignement of Bancroft *et al.*[3] based on a ligand field treatment including spin–orbit coupling, was $^2\Sigma_{1/2} < {}^2\Pi_{3/2} < {}^2\Delta_{5/2} < {}^2\Pi_{1/2} < {}^2\Delta_{3/2}$. Though the DFT calculations give a reasonable value for the absolute IE the ligand field treatment is undoubtedly superior for calculating relative state energies. The calculated 3d IEs quoted in Table 3 are for a δ hole where in

each case there is 99% localisation on the Zn. The calculations overestimate the Zn 3d binding energy by around 1 eV.

All three tabulated ionization bands show a decrease in IE in the order Me > Et > *neo*-Pe > *t*-Bu, *i.e.* with increasing values of the Taft *I* and *P* constants. This trend is open to interpretations in terms of destabilisation of the ground state orbitals with decreasing electron withdrawing power of the alkyl group, or in terms stabilisation of the excited, ionic state orbitals with increasing polarisability of R. Such considerations have been used successfully to account for the variations in ionisation and electron-attachment energies of substituted nickelocenes.[13] We have seen in the preceeding section that the ground state properties of the dialkylzincs are more strongly correlated with the *I* than with the *P* parameter. Polarisation effects are, however, likely to be more pronounced in the excited, ionic states. Plots of the σ_u and σ_g IEs against the Taft *I* and *P* parameters (Fig. 8) show that both sets of IEs correlate equally well with *I* and *P*, indicating that either or both effects are significant. The correlation for the 3d band is superior for *P*; removal of electron from an orbital completely localised on Zn presumably leads to a larger net positive charge on the metal atom and hence to a larger polarisation stabilisation.This interpretation is borne out by the fact that the calculated 3d orbital energies for the ground state only vary by 0.2 eV, whereas both the calculated and experimental IEs vary by between 0.6 and 0.7 eV (Table 3).

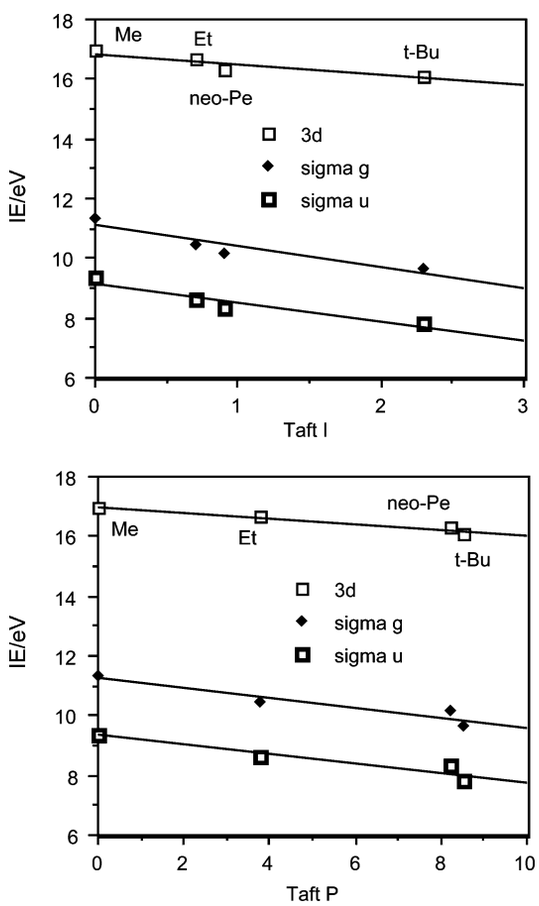

Fig. 8 Plot of σ_u and σ_g and Zn 3d ionisation energies for R_2Zn, R = Me, Et, *neo*-Pe and *t*-Bu against Taft inductive (*I*) and polarisability (*P*) constants. Linear correlation coefficients were for *I*, σ_u −0.95, σ_g −0.94 and 3d −0.90, and for *P*, σ_u −0.95, σ_g −0.94 and 3d −0.99.

Summary and concluding remarks

The mean Zn–C bond rupture enthalpy of dialkyl zinc compounds decreases significantly, while the Zn–C bond distance increases, with the number of methyl groups attached to the α-C atom. The introduction of methyl groups on the β-C atoms, on the other hand, has a much smaller effect. If it is assumed that the effect of Me groups bonded to the γ-C is insignificant, it follows that the strength of Zn–C bonds in dialkyl derivatives decreases in the order:

methyl > primary alkyl > secondary alkyl > tertiary alkyl (7a)

while the bond distance increases in the order:

methyl < primary alkyl < secondary alkyl < tertiary alkyl (7b)

Finally the Zn–C bonds in the silaneopentyl $(Me_3SiCH_2)_2Zn$ are shorter and stronger than those in *neo*-Pe_2Zn, and similar to the bonds in Me_2Zn. The observed variations cannot be due to steric interaction between the alkyl groups or to differences in the relaxation energies of the alkyl radicals, but may be attributed to decreasing polarity of the Zn–C bonds with decreasing electron-withdrawing power of the alkyl groups.

If this explanation is correct, one would expect the strength and length of M–C bonds in homoleptic alkyl derivatives of other metals to vary in the same manner, and there is indeed evidence to support this conclusion for alkyl derivatives of the main group metals in Groups 12, 13 and 14 and of the transition metals in Group 4, as revealed by the following findings.

(i) The mean M–C bond rupture enthalpies of Me_2Cd and Me_2Hg are larger than those of Et_2Cd and Et_2Hg, respectively, while that of Et_2Hg is in turn larger than that of *i*-Pr_2Hg.[5,9,14]

(ii) Similarly, the mean M–C bond rupture enthalpy of Me_3M is larger than that of Et_3M for M = B, Al or Ga.[5,14]

(iii) *D*(M–Me) is larger than *D*(M–Et) for M = Si, Ge, Sn or Pb.[5,14]

(iv) The M–C bonds in $(Me_3SiCH_2)_4M$ are stronger than those in $(Me_3CCH_2)_4M$ for M = Ti or Zr.[15]

Qualitative observations, such as the spontaneous rearrangement of *i*-Pr_3B and *i*-Pr_3Al to the corresponding tris-*n*-propyl derivatives, *n*-Pr_3B and *n*-Pr_3Al, respectively,[16,17] and of *t*-Bu_3B and *t*-Bu_3Al to the corresponding isobutyl derivatives,[17,18] show that bonds to a primary alkyl group are stronger than bonds to a secondary or a tertiary alkyl group. In these trisalkyls, as well as in the tetraalkyls of Group 4 or 14 elements, bonds to secondary alkyls, and particularly to tertiary alkyls, are presumably also destabilised by repulsion between the sterically more demanding ligands.

To the extent that the direction of insertion of alkenes into M–H or M–C bonds is determined by the thermodynamic stability of the products, the variation of bond strengths indicated by relation (7a) would imply that the metal atom will add to the olefin C atom bearing the larger number of H atoms. This is indeed the case in important reactions like the hydroboration of olefins,[19] or industrial processes like the dimerisation of propene as catalysed by *n*-Pr_3Al,[20] the polymerisation of propene as catalysed by $TiCl_3$ crystallites (Ziegler–Natta polymerisation),[21] or the hydrozirconation of α-alkenes by $Cp_2Zr(Cl)H$.[21]

Experimental and computational

Density functional theory calculations

The molecular structures of the dialkyl zinc compounds R_2Zn, R = Me, Et, *i*-Pr, *t*-Bu, *n*-Pr, *neo*-Pe or Me_3SiCH_2, of the hydrocarbons RH, and of the radicals R were optimised using the GAUSSIAN 98 program package,[22] with the B3LYP functional which incorporates Becke's exchange functional,[23] the local correlation functional of Vosko, Wilk and Nusair,[24] and the non-local correlation functional of Lee, Yang and Parr,[25,26] and a standard SDD basis. This basis set includes the Dunning/Huzinaga valence double-zeta basis set[27] for H, C and Si atoms, and a Stuttgart/Dresden ECP basis set[28] for Zn. In each case,

structure optimisation was followed by calculations of the molecular force field to ensure that a minimum on the potential energy surface had been found. The force fields were then transferred to the ASYM40 program[29] for calculation of root-mean-square vibrational amplitudes at the temperature of the electron diffraction experiments.

DFT calculations to support the interpretation of the photoelectron (PE) spectra were carried out using the Amsterdam Density Functional program.[30,31] The generalised gradient approximation was employed, with Becke's exchange functional,[23] the Vosko–Wilk–Nusair local correlation functional,[24] and non-local correlation corrections by Perdew.[32] Triple-zeta accuracy basis sets of Slater-type orbitals were used, with a single polarisation function added to the main group atoms. The cores of the atoms were frozen up to 1s for C, and 2p for Zn. First order relativistic corrections were made to the cores of all atoms. Relativistic corrections were made using the ZORA (Zero Order Relativistic Approximation) formalism. The ground state structures of Me_2Zn, Et_2Zn, *t*-Bu_2Zn and *neo*-Pe_2Zn were optimised. Vertical ionization energies were calculated by the ΔE method with the structures of the excited states assumed to be identical to those of the ground states.

Synthesis and characterisation

All manipulations were carried out using standard high-vacuum, Schlenk or glove-box techniques.[33] Diethylether, Mg turnings, Zn and Cu powders, and $ZnCl_2$ (Aldrich) were dried by established methods.[33] MeI and EtI (Aldrich) were converted to Me_2Zn and Et_2Zn, respectively, by reaction with a zinc/copper couple at 120 °C.[34] *i*-PrBr, *t*-BuBr, *neo*-PeBr and Me_3SiCH_2Br (Aldrich) were each converted to the corresponding Grignard or alkyllithium reagent by reaction with magnesium or lithium (Aldrich) metal in Et_2O, and thence to the corresponding dialkylzinc by reaction with anhydrous $ZnCl_2$.[35] In each case, the dialkylzinc produced was characterised by reference to its ^1H, ^{13}C and [for $(Me_3SiCH_2)_2Zn$] ^{29}Si NMR spectrum in either $CDCl_3$ or C_6D_6 solution.

Gas electron diffraction

The gas electron diffraction data for *i*-Pr_2Zn, *t*-Bu_2Zn, *neo*-Pe_2Zn and $(Me_3SiCH_2)_2Zn$ were recorded on the Baltzers KDG2 unit at the University of Oslo[36] with an all-glass inlet system at ambient temperatures and nozzle-to-plate distances of approximately 50 and 25 cm. Further information about the experiments is summarised in Table 4. Atomic scattering factors were taken from ref. 37. Backgrounds were drawn as least-squares adjusted polynomials to the difference between the total experimental and calculated molecular intensities.

Structure refinements

Structure refinements were carried out by least-squares calculations on the molecular intensities using the program KCED 26 written by Gundersen, Samdal, Seip and Strand.[38] Non-refined vibrational amplitudes were fixed at calculated values. Corrections for thermal vibration were neglected. Since the refinements were carried out with diagonal weight matrices, the estimated standard deviations listed in Table 1 have been doubled to include uncertainty due to data correlation[39] and expanded to include a scale uncertainty of 0.1%.

Structure refinements for *t*-Bu_2Zn were carried out on a molecular model of D_3 symmetry. This means that the structure of the ZnC_8 frame is determined by four independent parameters, *viz*. the Zn–C, and C–C bond distances, the valence angle ∠ZnCC and the dihedral angle $\tau(C_\beta C_\alpha C_\alpha' C_\beta')$, All C–$CH_3$ fragments were assumed to have local C_{3v} symmetry. The position of the H atoms is then fixed by three additional independent parameters, *viz*. the C–H bond distance, the ∠CCH valence angle and one dihedral angle of the type τ(ZnCCH). Least-squares refinement of the seven structure parameters and twelve r.m.s. vibrational amplitudes yielded the *R*-factors listed in Table 3. The best values for the framework parameters are given in Table 1. The H atom structure parameters of this and all the other molecules under investigation were unexceptional and are therefore not listed. Calculated and observed radial distribution curves are compared in Figure 2. We consider the agreement satisfactory.

Structure refinements of *i*-Pr_2Zn were based on a molecular model of C_2 symmetry. This means that the structure of the ZnC_6 frame is determined by six independent parameters, *viz*. the Zn–C and C–C bond distances, the valence angles ∠CZnC, ∠ZnCC and ∠CCC and the dihedral angle τ(HC(1)-C(11)H) which determines the relative positions of the two alkyl groups. The positions of the methyl group H atoms were again determined by three parameters, the C–H bond distance, the ∠CCH valence angle and one dihedral angle τ(ZnCCH). Finally, the C(1)–H bond distance was assumed equal to the methyl group bond distance, the valence angle ∠ZnC(1)H fixed at the calculated value (106.6°) and the ZnC(1)H plane assumed to bisect the ∠CCC angle. Refinement of the nine structure parameters and nine vibrational amplitudes yielded the structure parameters listed in Table 1 and an *R*-factor of 3.5%.

Structure refinements of *neo*-Pe_2Zn were based on a molecular model of C_2 symmetry, (see Fig. 1). The structure of the ZnC_{10} frame of the molecule is then determined by fourteen independent parameters. This number was reduced by assuming that the C_5 skeleton of each *neo*-pentyl group has C_s symmetry, with the C atoms 1, 2 and 4 in the mirror plane as suggested by the DFT calculations, and by fixing the small differences between individual C–C bond distances (1.1 pm or less) at the calculated values. Finally, we assumed all C–CH_3 fragments to have C_{3v} symmetry, fixed the difference between C_α–H and C_γ–H bond distances at the calculated value, and transferred the angles fixing the positions of the H atoms on C_α from the calculated structure. The molecular structure is then determined by eleven parameters: the Zn–C bond distance, the mean C–C and C–H bond distances, the valence angles ∠CZnC, ∠ZnCC, ∠C(1)C(2)C(3), ∠C(1)C(2)C(4), ∠C(3)C(2)C(5) and $\angle C_\beta C_\gamma H$, and the two dihedral angles $\tau(C_\beta C_\alpha C_\alpha' C_\beta')$ and $\tau(ZnC_\alpha C_\beta C_\gamma)$. Refinement of eleven structure parameters and ten vibrational amplitudes yielded the structure parameters listed in Table 1.

The refinement scheme adopted for the sila-substituted *neo*-pentylzinc compound, $(Me_3SiCH_2)_2Zn$ was very similar, but in order to obtain convergence it proved necessary to reduce the number of unknown structure parameters to nine by fixing the valence angles ∠C(1)Si(2)C(4) and ∠C(3)Si(2)C(5) at the calculated values. The number of refined vibrational amplitudes was reduced to seven.

Photoelectron spectroscopy

PE spectra of R_2Zn, R = Me, Et, *n*-Pr or *t*-Bu, were measured using a PES Laboratories 0078 spectrometer interfaced with an Atari microprocessor. The samples were held at room temperature external to the spectrometer and the vapour pressure in the chamber controlled with a needle valve. Spectral acquisition was by repeated scans. The spectra were calibrated with He, Xe and N_2.

Acknowledgements

The quantum chemical calculations were carried out at the facilities of the High Performance Computing Centre at the University of Oslo, the Super-Computing centre at Oxford, and the EPSRC Columbus cluster at the Rutherford Laboratory. A. H. is grateful to Professor Einar Uggerud, University of Oslo, for a helpful discussion. Thanks are also due to Jesus College of Oxford for a research fellowship (to G. S. M.), to

Table 4 Gas electron diffraction (GED) data collection and structure refinements

Compound	*i*-Pr_2Zn	
Detector plates	KODAK [a]	
Nozzle temperature/°C	23 ± 3	
Nozzle to plate distance/cm	50	25
No. of plates	5	6
$s_{min}/s_{max}/\Delta s$ (nm^{-1})	18.75/147.50/1.25	42.5/245.0/2.5
Least-squares weights	1.00	1.00
R-factors [c]	0.028	0.049
No. of refined structure parameters	9	
No. of refined amplitudes	9	
Compound	*t*-Bu_2Zn	
Detector plates	KODAK [a]	
Nozzle temperature/ °C	23 ± 3	
Nozzle to plate distances/cm	50	25
No. of plates	6	6
$s_{min}/s_{max}/\Delta s$ (nm^{-1})	21.25/151.25/1.25	62.5/300.0/2.5
Least-squares weights	1.00	1.00
R-factors [c]	0.030	0.053
No. of refined structure parameters	7	
No. of refined amplitudes	12	
Compound	*neo*-Pe_2Zn	
Detector plates	FUJI [b]	
Nozzle temperature/ °C	23 ± 3	
Nozzle to plate distances/cm	50	25 [d]
No. of plates	3	3
$s_{min}/s_{max}/\Delta s$ (nm^{-1})	17.50/153.75/1.25	40.0/225.0/2.5
Least-squares weights	1.00	1.00
R-factors [c]	0.046	0.052
Nozzle to plate distances/cm	25 [d]	25 [d]
No. of plates	2	3
$s_{min}/s_{max}/\Delta s$	45.0/225.0/2.5	45.0/282.5/2.5
Least-squares weights	1.00	0.35
R-factors [c]	0.053	0.088
No. of refined structure parameters	11	
No. of refined amplitudes	10	
Compound	$(Me_3SiCH_2)_2Zn$	
Detector plates	FUJI [b]	
Nozzle temperature/ °C	23 ± 3	
Nozzle to plate distances/cm	50	25
No. of plates	3	3
$s_{min}/s_{max}/\Delta s$ (nm^{-1})	28.75/153.75/1.25	55.0/280.0/2.5
Least-squares weights	1.00	0.20
R-factors [c]	0.015	0.061
No. of refined structure parameters	9	
No. of refined amplitudes	7	

[a] KODAK Electron Image plates. [b] FUJI Imaging Plates BAS-III. [c] $R = \sqrt{[\Sigma w(I_{obs} - I_{calc})^2/\Sigma w I_{obs}^2]}$. [d] Three data sets were recorded for *neo*-Pe_2Zn with a nozzle to plate distance of 25 cm before we succeeded in obtaining data beyond $s = 220$ nm^{-1}.

King's College London for a studentship (to E. G.), to EPSCR for provision of glove-box facilities, and to Julia Nice for assitance with some of the syntheses.

References and notes

1 D. Seyferth, *Organometallics*, 2001, **20**, 2940.
2 K. S. Rao, B. P. Stoicheff and R. Turner, *Can. J. Phys.*, 1960, **38**, 1516.
3 G. M. Bancroft, D. K. Creber, M. A. Ratner, J. W. Moskowitz and S. Topiol, *Chem. Phys. Lett.*, 1977, **50**, 233.
4 A. Almenningen, T. U. Helgaker, A. Haaland and S. Samdal, *Acta Chem. Scand., Ser. A*, 1982, **36**, 159.
5 G. Pilcher and H. A. Skinner, in *The Chemistry of the Metal–carbon Bond*, ed. F. R. Hartley and S. Patai, Wiley, New York, 1982, vol. 1, p. 43.
6 H. Y. Afeefy, J. F. Liebmann and S. E. Stein, *Neutral Thermochemical Data*, in NIST Chemistry WebBook, NIST Standard Reference Database Number 69 – July 2001 Release, ed. W. G. Mallard and P. J. Lindstrom, National Institute of Science and Technology, 2001; http://webbook.nist.gov/chemistry.
7 J. B. Pedley and J. Rylance, Sussex-N.P.L. Computer Analysed Thermochemical Data, University of Sussex, Brighton, 1977.
8 I. E. Gümrükçüoglü, J. Jeffery, M. F. Lappert, J. B. Pedley and A. K. Rai, *J. Organomet. Chem.*, 1988, **341**, 53.
9 G. Pilcher, *Pure Appl. Chem.*, 1989, **61**, 855.
10 D. W. Smith, *J. Organomet. Chem.*, 1999, **585**, 150.
11 A study of 40 singly bonded gaseous heteronuclear diatomic molecules AB, (*viz*. four hydrogen halides HX, six interhalogen compounds XX′, five alkali metal hydrides MH, five inter alkali metal compounds MM′, and 20 alkali metal halides MX) shows that the observed bond distances *r*(A–B) are either approximately equal to, or shorter than, the arithmetic mean of the bond distances in the homonuclear compounds (A_2 and B_2), *i.e.* that

$$r(A–B) \leq (1/2)[r(A–A) + r(B–B)]$$

and that the difference increases with increasing electronegativity difference, $\Delta\chi = |\chi_A - \chi_B|$. Similarly, the the bond enthalpy *D*(A–B) is either approximately equal to, or larger than, the geometric mean of the bond enthalpies of the homonuclear compounds

$$D(A–B) \leq \sqrt{[D(A–A)D(B–B)]}$$

the difference increasing with $\Delta\chi$. A. Haaland, unpublished results.
12 R. W. Taft, M. Taagepera, J. L. M. Abboud, J. F. Wolf, D. J. DeFrees, W. J. Hehre, J. E. Bartmess and R. T. McIver, Jr., *J. Am. Chem. Soc.*, 1978, **100**, 7765 . The inductive and polarisability parameters are as follows: Me: $I = 0.0$, $P = 0.0$; Et: $I = 0.7$, $P = 3.8$; *i*-Pr: $I = 1.5$, $P = 6.5$; *t*-Bu: $I = 2.3$, $P = 8.5$; *n*-Pr: $I = 0.9$, $P = 5.6$; *neo*-Pe: $I = 0.9$, $P = 8.2$. Corresponding values for Me_3SiCH_2 do not appear to have been evaluated.

13 D. E. Richardson, M. F. Ryan, Md. N. I. Khan and K. A. Maxwell, *J. Am. Chem. Soc.*, 1992, **114**, 10482.
14 H. A. Skinner and J. A. Connor, *Pure Appl. Chem.*, 1985, **57**, 79.
15 M. F. Lappert, D. S. Patil and J. B. Pedley, *Chem. Commun*, 1975, 830.
16 R. Köster, in *Progress in Boron Phemistry*, ed. H. Steinberg and A. L. McClosky, Pergamon Press, London, 1964, vol. 1, p. 289.
17 T. Mole and E. A. Jeffery, *Organoaluminium Compounds*, Elsevier, Amsterdam, 1972, p 119.
18 H. Nöth and T. Taeger, *J. Organomet. Chem.*, 1977, **142**, 281.
19 H. C. Brown, Boranes in Organic Chemistry, Cornell University Press, Ithaca, NY, 1972.
20 G. E. Coates and K. Wade, *Organometallic Compounds*, Vol. 1, *The Main Group Elements*, Methuen, London, 1967, p. 321.
21 F. A. Cotton, G. Wilkinson, C. A. Murillo and M. Bochmann, *Advanced Inorganic Chemistry*, Wiley, New York, 6th edn., 1999, pp. 1222 and 1270.
22 Gaussian 98, revision A.7, M. J. Frisch, G. W. Trucks, H. B. Schlegel, G. E. Scuseria, M. A. Robb, J. R. Cheeseman, V. G. Zakrzewski, J. A. Montgomery, Jr., R. E. Stratmann, J. C. Burant, S. Dapprich, J. M. Millam, A. D. Daniels, K. N. Kudin, M. C. Strain, O. Farkas, J. Tomasi, V. Barone, M. Cossi, R. Cammi, B. Mennucci, C. Pomelli, C. Adamo, S. Clifford, J. Ochterski, G. A. Petersson, P. Y. Ayala, Q. Cui, K. Morokuma, D. K. Malick, A. D. Rabuck, K. Raghavachari, J. B. Foresman, J. Cioslowski, J. V. Ortiz, A. G. Baboul, B. B. Stefanov, G. Liu, A. Liashenko, P. Piskorz, I. Komaromi, R. Gomperts, R. L. Martin, D. J. Fox, T. Keith, M. A. Al-Laham, C. Y. Peng, A. Nanayakkara, C. Gonzalez, M. Challacombe, P. M. W. Gill, B. Johnson, W. Chen, M. W. Wong, J. L. Andres, M. Head-Gordon, E. S. Replogle and J. A. Pople, Gaussian, Inc., Pittsburgh PA, 1998.
23 A. D. Becke, *Phys. Rev. A*, 1988, **38**, 3098.
24 S. H. Vosko, L. Wilk and M. Nusair, *Can. J. Phys.*, 1980, **58**, 1200.
25 C. Lee, W. Yang and R. G. Parr, *Phys. Rev. B*, 1988, **37**, 785.
26 B. Miehlich, A. Savin, H. Stoll and H. Preuss, *Chem. Phys. Lett.*, 1989, **157**, 200.
27 T. H. Dunning, Jr. and P. J. Hay, in *Modern Theoretical Chemistry*, ed. H. F. Schaefer, III, Plenum, New York, 1976, p 1.
28 M. Dolg, U. Wedig, H. Stoll and H. Preuss, *J. Chem. Phys.*, 1987, **86**, 866.
29 L. Hedberg and I. M. Mills, *J. Mol. Spectrosc.*, 1993, **160**, 117.
30 ADF Program System, Release 2000.02, Scientific Computing and Modeling NV, Vrije Universiteit; Theoretical Chemistry, De Boelelaan 1083, 1081 HV Amsterdam, The Netherlands. A description of the program system is found in the following publications: E. J. Baerends, D. E. Ellis and P. Ros, *Chem. Phys.*, 1973, **2**, 41; L. Versluis and T. Ziegler, *J. Chem. Phys.*, 1988, **88**, 322; C. Fonseca Guerra, J. G. Snijders, G. te Velde and E. J. Baerends, *Theor. Chem. Acc.*, 1998, **99**, 391.
31 G. te Velde and E. J. Baerends, *J. Comput. Phys.*, 1992, **99**, 84.
32 J. P. Perdew, *Phys. Rev. B*, 1986, **33**, 8822; J. P. Perdew, *Phys. Rev. B*, 1986, **34**, 7406.
33 D. F. Shriver and M. A. Drezdzon, *The Manipulation of Air-Sensitive Compounds*, Wiley, New York, 2nd edn., 1986.
34 C. R. Noller, *Org. Synth.*, 1943, **Coll. vol. II**, 184.
35 R. R. Schrock and J. D. Fellmann, *J. Am. Chem. Soc.*, 1978, **100**, 3359; S. Moorhouse and G. Wilkinson, *J. Chem. Soc., Dalton Trans.*, 1974, 2187; J. M. Huggins, D. R. Whitt and L. Lebioda, *J. Organomet. Chem.*, 1986, **312**, C15; M. Westerhausen, B. Rademacher and W. Poll, *J. Organomet. Chem.*, 1991, **421**, 175.
36 W. Zeil, J. Haase and L. Wegmann, *Z. Instrumentenk.*, 1966, **74**, 84.
37 A. W. Ross, M. Fink and R. L. Hilderbrandt, in *International Tables for Crystallography*, ed. A. J. C. Wilson, Kluwer Academic Publishers, Dordrecht, 1992, Vol. C, p. 245.
38 G. Gundersen, S. Samdal, H. M. Seip and T. G. Strand, KCED26, Department of Chemistry, University of Oslo, 1996.
39 H. M. Seip, T. G. Strand and R. Stølevik, *Chem. Phys. Lett.*, 1969, **3**, 617.